ACTA CHEMICA SCANDINAVICA 26 (1972) 175–190

Neutron Diffraction Investigations on Quenched MnBi and $MnBi_{0.9}Sb_{0.1}$

A. F. ANDRESEN, J. E. ENGEBRETSEN and J. REFSNES

Institutt for Atomenergi, Kjeller, Norway

It has been found that the orthorhombic MnBi phase which is obtained on quenching from above 360°C can be produced as a stable phase at low temperature by the addition of a small amount of antimony. Some of the Mn-atoms occupy interstitial positions and an ordering is found to take place both with respect to the vacancies and the interstitials. Vacancies also occur in the Bi-lattice. In $MnBi_{0.9}Sb_{0.1}$ moments of magnitude 2.0 μ_B form a spiral structure propagating along the *c*-axis. The Néel temperature is 195 ± 3 K. In quenched MnBi moments of magnitude 2.50 μ_B lie on cones around the *c*-axis with approximate opening angle 90°. The ferromagnetic component along the *c*-axis is 1.73 μ_B.

At room temperature MnBi is ferromagnetic with a saturation moment of 4.5 μ_B per Mn-atom.[1] The structure is hexagonal of the NiAs type and the moments point along the hexagonal *c*-axis. On heating to above 360°C there is a first order transition to a paramagnetic state in which several of the Mn-atoms occupy interstitial positions. Upon rapid quenching some of these are retained at low temperature and a new ferromagnetic phase appears. This has an orthorhombic supercell and from magnetization measurements a ferromagnetic saturation moment of only 1.7 μ_B per Mn-atom.[2] In a previous neutron diffraction investigation [1] one of the authors found that this value could be explained by assuming that the moments on the interstitial atoms have an antiparallel alignment and that some of the other Mn-atoms are in a low spin state. However, due to the small number of superreflections observed and the low resolution of the diagrams, it was not possible to arrive at any definite conclusions for either the chemical or the magnetic structure of the quenched phase. The quenching was never rapid enough to produce a complete transition, and even at room temperature the orthorhombic phase would slowly transform back to the hexagonal phase.

In MnAs a similar transition from a ferromagnetic NiAs-type phase to a paramagnetic, orthorhombic, MnP-type phase is observed at 42.6°C.[3,4] Goodenough *et al.*[5] found that the characteristic magnetic differences between

these phases can be explained as a transition from a high spin state in the hexagonal phase to a low spin state in the orthorhombic phase. On studying the system $MnAs_{1-x}P_x$ they found that the substitution of the smaller anion phosphorus for arsenic had the effect of stabilizing the orthorhombic structure. Substitution with the larger anion antimony had the opposite effect. By applying a pressure Goodenough and Kafalas [6] were indeed able to show that the transition from a hexagonal to an orthorhombic phase is coupled to a critical molar volume.

Although MnBi does not transform to an MnP type structure the situation seems to be very similar. The low observed moment in the orthorhombic phase is in agreement with a low spin state as proposed by Goodenough *et al.* In analogy one could assume the existence of a critical molar volume also here and that the substitution of the smaller anion antimony for bismuth would have the effect of stabilizing the orthorhombic phase. Changes in the interatomic distances would result in changes in the magnetic exchange interactions and possibly lead to a better understanding of the magnetic ordering. Furthermore, if a stable phase were obtained, a study could also be made of the temperature dependence of its magnetic properties.

We therefore decided to study the system $MnBi_{1-x}Sb_x$ in combination with a renewed investigation of quenched MnBi. This investigation would benefit not only from the increased resolution and intensity now available in the neutron diffraction diagrams, but also from the availability of the least squares profile refinement program [7] making it possible to utilize all the information contained in a powder diffraction diagram.

EXPERIMENTAL

The materials used in the preparations were electrolytic grade manganese (British Drug Houses Ltd.) with purity better than 99.9 %, bismuth from Koch-Light Laboratories Ltd., purity 99.999 %, and antimony from the same manufacturer, purity 99.9995%. Accurately weighed quantities of the constituents were ground under argon atmosphere and sealed in evacuated silica tubes. To improve the contact between the components some of the samples were first pressed to pellets under a pressure of 10 tons/cm^2.

For the MnBi samples two different heating procedures were used. In one the samples were slowly heated to 430°C and kept between 430° and 440°C for two to three weeks. The decomposition point of MnBi is 445°C. The difficulty in obtaining a complete reaction is the formation of a stoichiometric surface layer on the manganese grains, but by keeping a reaction temperature close to the decomposition point the diffusion rate may be enhanced. In another procedure the samples were, in accordance with a suggestion of Cornish,[8] heated to 262°C, just below the melting point of bismuth. At this temperature a liquid eutectic is thought to form at the interface of the manganese and bismuth particles. MnBi is then formed by solid state diffusion. During the reaction the temperature was slowly increased to above the melting point of bismuth, 271°C. In both cases the heating procedure was repeated after opening the tubes and grinding the samples. However, little was attained on repeated heatings. In neither case was it possible to obtain pure stoichiometric samples. The best result was obtained with a combination of the two heat treatments, *i.e.* heating first to 262°C and then, after slow heating, keeping the temperature for a longer period at about 435°C. However, the final product always contained some unreacted Bi and usually a slight amount of MnO. Before quenching the samples were first divided in small batches, less than 5 g, and sealed in thin-walled silica tubes. They were heated to above 380°C and rapidly quenched in ice water. The completeness of the quenching was checked with X-rays for each batch separately. The process of heating and quenching always led to a larger amount of unreacted bismuth. Besides a

small amount of a phase identified as Mn_2Bi_3 was formed. This phase which is orthorhombic and ferromagnetic was previously found by Fürst and Halla [9] and Halla and Montignié [10] in samples quenched from high temperatures.

According to Dannöhl and Gmöhling [11] there is a complete miscibility of MnBi and MnSb at the stoichiometric composition Mn:(Bi+Sb) = 1:1. However, with an increasing content of Sb it proved difficult to avoid the formation of Mn_2Sb. As it was found sufficient for stabilizing the orthorhombic structure to add 5 at. % Sb, only samples with a small amount of Sb were studied. A good sample with a minimum of impurities was obtained at the composition $MnBi_{0.9}Sb_{0.1}$. The impurities were, aside from unreacted Bi and α-Mn, small amounts of Mn_2Sb and MnO. It is the results on this sample which will be treated in this paper.

The neutron diffraction diagrams were obtained at the JEEP II reactor using neutrons of wavelength 1.863 ± 0.002 Å reflected from the (111)-planes of a pressed germanium monochromator crystal. In this case a long wavelength could be used without getting an excessive contamination of $\lambda/2$ neutrons since the 222-reflection of germanium is extinguished. Still a weak 222-reflection is present due to multiple scattering in the monochromator, and the monochromatized beam contains a small amount of both $\lambda/2$ and $\lambda/3$ neutrons. Where needed the observed intensities have been corrected for this contamination.

For the low temperature runs a liquid helium cryostat manufactured by Cryogenic Associates was used. The temperature was recorded with calibrated platinum and germanium resistance thermometers and the temperature could be stabilized to $\pm 0.2°$. Due to a heat leak between the liquid helium and the liquid nitrogen level the liquid helium temperature could not be reached, and for the lowest temperature runs the temperature was stabilized at 12°K.

Two different least squares programmes were used in determining the structural parameters. For the X-ray case, where integrated intensities were observed, we used a full matrix least squares programme written by Begum and Satya Murthy.[12] For the neutron data on the other hand, the profile refinement programme of Rietveld [7] could be employed. This is based on the observed intensity in each experimental point and performs a simultaneous refinement on both the nuclear and magnetic parameters. It is assumed that the peaks have a Gaussian shape, which has been found to be closely true for the peaks in our diagrams, and that their half width, H_K, varies according to the expression:

$$H_K^2 = U \tan^2 \theta_K + V \tan \theta_K + W$$

Here U, V, and W are parameters whose initial values can be determined by a separate least squares programme.

The obtained agreement is given by a reliability factor defined as:

$$R_{nucl} = 100 \sum_i |F_i^2(obs) - (1/c)F_i^2(nucl)| / \sum_i F_i^2(obs)$$

for the nuclear reflections, and

$$R_{magn} = 100 \sum_i |F_i^2(obs) - (1/c)F_i^2(magn)| / \sum_i F_i^2(obs)$$

for the magnetic reflections.

The calculated standard deviations of the parameters are in each case appended in brackets.

ROOM TEMPERATURE MEASUREMENTS ON $MnBi_{0.9}Sb_{0.1}$

Apart from the impurity peaks due to Bi, α-Mn, MnO, and Mn_2Sb all the observed peaks both in the X-ray and neutron diffraction diagrams obtained at room temperature could be indexed on an orthorhombic unit cell of the dimensions given in Table 1. This unit cell can be considered derived from an hexagonal cell with $a_0 = 4.30$ Å and $c_0 = 5.74$ Å by making $a \approx a_0$, $b \approx \sqrt{3}\, a_0$ and $c \approx c_0$. It is similar to the unit cell of quenched MnBi previously [1] deduced,

Table 1. Unit cell dimensions of $MnBi_{0.9}Sb_{0.1}$.

	a	*b*	*c*
12 K	4.274(3)	7.409(5)	5.718(3)
293 K	4.304(5)	7.449(4)	5.742(4)

but with no doubling of the *a* and *c* axes. The same superreflections are observed, only in this case they are stronger and additional ones also appear. Thus by adding antimony it has been possible not only to make the orthorhombic phase the stable phase at room temperature, but to make the superstructure appear more clearly.

The presence of superreflections violating the space group conditions of *Pnma* made it clear that the superstructure was not of the MnP-type. A thorough search of all the orthorhombic space groups showed $P222_1$ to be the only one which, while allowing all the observed reflections, made it possible to accomodate all the atoms belonging to an NiAs-like lattice. The corresponding atomic positions are given in Table 2. In analogy to quenched MnBi some

Table 2. Atomic positions in $MnBi_{0.9}Sb_{0.1}$. Space group $P222_1 - D_2^2$.

2 Mn_1 in (*a*)	$x,0,0;\bar{x},0,\frac{1}{2}$
2 Mn_2 in (*b*)	$x,\frac{1}{2},0;\bar{x},\frac{1}{2},\frac{1}{2}$
2 $Mn(I)_1$ in (*c*)	$0,y,\frac{1}{4};0,\bar{y},\frac{3}{4}$
2 $Mn(I)_2$ in (*d*)	$\frac{1}{2},y,\frac{1}{4};\frac{1}{2},\bar{y},\frac{3}{4}$
2 Bi/Sb_1 in (*c*)	$0,y,\frac{1}{4};0,\bar{y},\frac{3}{4}$
2 Bi/Sb_2 in (*d*)	$\frac{1}{2},y,\frac{1}{4};\frac{1}{2},\bar{y},\frac{3}{4}$

of the Mn-atoms were assumed to occupy the trigonal bipyramidal holes of the NiAs-type structure. These positions are denoted Mn(I). A *c*-axis projection of the unit cell is shown in Fig. 1a, the dashed lines giving the projection of the related hexagonal cell.

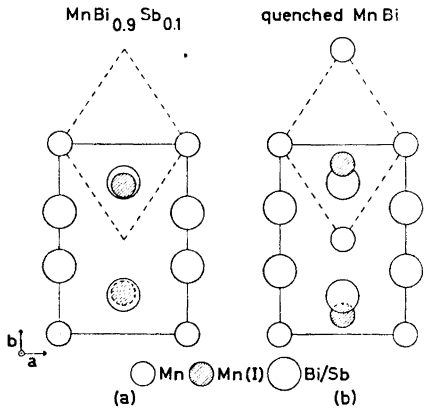

Fig. 1. *c*-Axes projection of the unit cell of $MnBi_{0.9}Sb_{0.1}$ (a) and quenched MnBi (b). Dashed lines give the projection of the related hexagonal cell.

Treating first the X-ray data a least squares refinement was carried out on the integrated intensity of 19 resolved X-ray peaks using the least squares programme written by Begum and Satya Murthy.[12] Both the position parameters and the occupation numbers, defined as the fraction of a position occupied by an atom, were varied together with the scale factor. The temperature parameter was kept constant at $B = 0.5$ Å^2 for all atoms. It soon appeared that the occupation number of the (*b*) position rapidly converged to zero, and this position was therefore omitted. This means that all the Mn-atoms in the row passing through the centre of the cell have moved into interstitial positions. The interstitial atoms seemed to occupy mainly the (*d*) position, which had an occupation number of 0.84, whereas the (*c*) position had an occupation number of only 0.21. The refinement was continued until negligible shifts were obtained and led to a final *R*-factor of 10.3 %.

A more reliable refinement could be carried out on the neutron diffraction data using the profile refinement programme of Rietveld.[7] As starting parameters were used the values obtained from the refinement of the X-ray data. It soon appeared that also the occupation number of the (c) position of Mn(I) approached zero, and this position was also omitted. This means that perpendicular to the *a*-axis (Fig. 1a) every second layer contains Mn-atoms only in interstitial positions, and every second only in regular positions. This has important consequences for the atomic displacements. The only *x*-parameter adjustable, that for Mn_1 in (a), remained close to zero and had standard deviations larger than its value. In the later refinements it was therefore fixed at zero. The occupation number of this position remained close to unity and was finally fixed at this value. The other occupation numbers, the *y*-parameters, the scale-factor, the overall isotropic temperature parameter, the lattice parameters and the three profile parameters were refined until negligible shifts were obtained. The final values for the occupation numbers, the *y*-parameters and the isotropic temperature parameters are given in Table 3. The final *R*-factor was 4.7 %.

It appears that vacancies are also present in the Bi positions and about equally distributed over the two available sites. The sum of the occupation numbers of the Bi and Mn positions is such as to give a close to equiatomic composition. We have assumed that the Sb-atoms are randomly distributed over the Bi-sites and for the scattering amplitude we have used $b_{Bi/Sb} = 0.824 \times 10^{-12}$ cm based on the values $b_{Bi} = 0.864 \times 10^{-12}$ cm and $b_{Sb} = 0.54 \times 10^{-12}$ cm.[13] For Mn the value $b_{Mn} = -0.36 \times 10^{-12}$ cm was used.

Table 3. Result of least squares profile refinement calculations on $MnBi_{0.9}Sb_{0.1}$.

	293 K				12 K			
	occ.no.	*x*	*y*	*z*	occ.no.	*x*	*y*	*z*
Mn in (*a*)	1	0	0	0	1	0	0	0
Mn(I) in (*d*)	0.38(3)	½	0.215(8)	¼	0.40(2)	½	0.210(7)	¼
Bi/Sb in (*c*)	0.69(3)	0	0.359(4)	¼	0.63(1)	0	0.361(4)	¼
Bi/Sb in (*d*)	0.65(2)	½	0.796(4)	¼	0.66(1)	½	0.797(3)	¼
Overall isotropic *B*	0.52(21) Å^2				0.18(18) Å^2			
R_{nucl}	4.7 %				7.9 %			

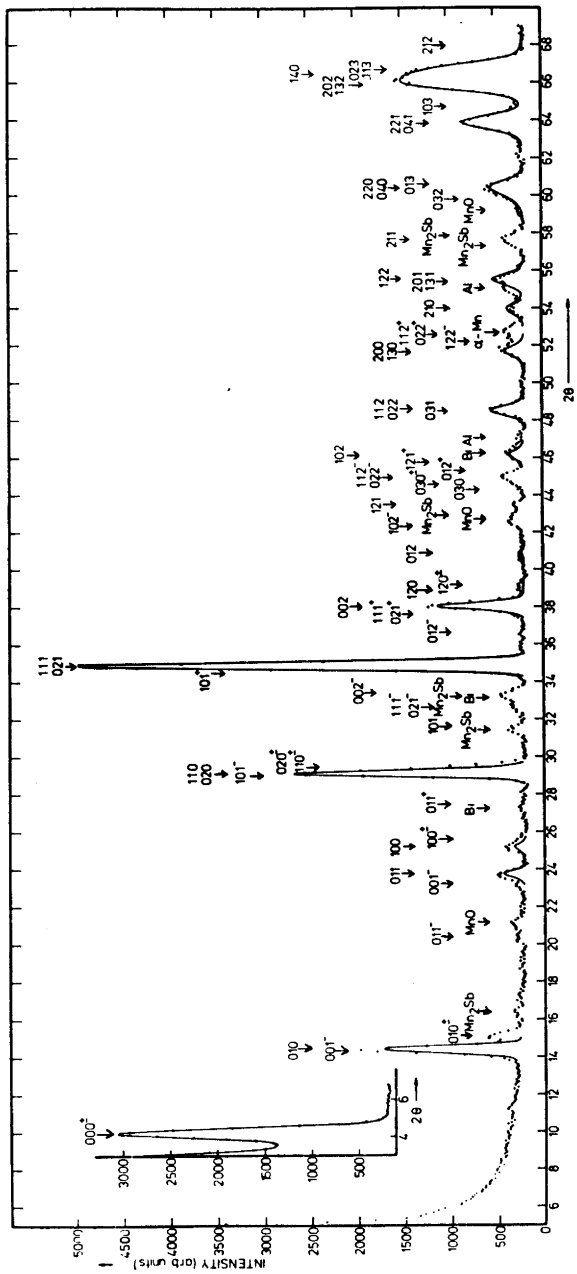

Fig. 2. Neutron diffraction diagram of $MnBi_{0.9}Sb_{0.1}$ obtained at 12 K, $\lambda = 1.863$ Å. The fully drawn curve is the result of a least squares profile refinement calculation excluding satellites. Insert shows the low angle part of the diagram repeated with narrow collimation. The curve is drawn through the experimental points.

LOW TEMPERATURE RESULTS ON $MnBi_{0.9}Sb_{0.1}$.

For the lowest temperature runs (see above) the temperature was stabilized at 12 ± 0.2 K. A neutron diffraction diagram obtained at this temperature is shown in Fig. 2. This has a number of additional peaks which cannot be indexed on any supercell derived by a reasonable enlargement of the chemical unit cell. Using a narrow collimation a strong peak was also observed close to the primary beam at $2\theta = 4.37°$ (see insert in Fig. 2). This can be assumed to be the $000^{\pm}$ satellite due to a spiral structure, and in fact both this and all the other extra peaks can be indexed as satellites due to spirals propagating along the c^* axis with a propagation vector $0.228\ \vec{c}^*$. The absence of any higher order satellites rules out the possibility of an antiphase domain structure. The integrated intensities of the observed satellite peaks are given in Table 4.

Table 4. Satellite intensities of $MnBi_{0.9}Sb_{0.1}$.

	12 K			78 K		
hkl	I_{calc} $\mu = 2.0$		I_{obs}	I_{calc} $\mu = 1.7$		I_{obs}
$000^{\pm}$	411.65		441.3	369.51		378.4
$010^{\pm}$	21.05		16.9	19.45		15.0
011^{-}	6.40		4.2	1.72		0.8
001^{+}	1.97		3.6	0.00		–
$100^{\pm}$	1.45		2.5	1.67		2.3
011^{+}	3.41		2.4	0.98		0.9
111^{-}	3.07			0.88		
021^{-}	1.24	4.31	6.9	0.10	0.98	1.3
$120^{\pm}$	5.72		4.2	5.44		3.6
$030^{\pm}$	0.60			0.54		
022^{-}	3.04			2.79		
112^{-}	4.00	9.07	12.0	3.69	8.48	11.9
012^{+}	1.43			1.45		

On heating to 78 K the satellites remain in approximately the same positions; however, as seen in Table 4 some of the intensities have changed. In particular the intensities of the peaks 011^{-}, 001^{+}, 011^{+}, and the combined 111^{-}, 021^{-} have been drastically reduced. This cannot be explained from any changes in the atomic positions or the moment values, but can be ascribed to a change in the phase relations between the spirals running through the different metal sites.

There are four Mn-atoms per unit cell through which different spirals may run. The intensity of the satellites depends on the phase difference, ϕ_j, between these spirals through the relation

$$I_{\vec{H} \pm \vec{\tau}} = Kp^2 \frac{1 + (\vec{e} \times \vec{z})^2}{4} \{\sum_j \mu_j \sin \beta_j f(\vec{H} \pm \vec{\tau}) \exp i(2\pi \vec{H} \vec{r}_j \mp \phi_j)\}^2$$

Here $\vec{H}$ is a reciprocal lattice vector and $\vec{\tau}$ is the spiral propagation vector. K is a scale factor and p the magnetic scattering amplitude. $\vec{e}$ is the unit vector in direction of the scattering vector and $\vec{z}$ the unit vector in direction of the spiral axis. The summation is over all the magnetic atoms in the unit cell which have position vectors $\vec{r}_j$ and magnetic moment μ_j forming an angle β_j with the spiral axis. β_j is here taken as equal to 90° as there is no sign of any magnetic contribution to the fundamental peaks. f is the magnetic form factor, and for this we have used in accordance with previous results [1] the form factor for Mn^{3+} calculated by Watson and Freeman.[14]

A computer programme was made which enabled us to calculate the intensity of all the observed satellites letting ϕ_j run through a set of predetermined values. For each set the reliability factor R, defined as above, was calculated. With the data observed at 78 K a minimum of R was obtained with all the spirals in phase. Using the normalization factor obtained for the fundamental reflections and assuming the same moment for all the atoms a moment value of 1.7 μ_B was deduced. The agreement obtained is shown in Table 4.

The intensity changes observed at 12 K cannot be explained as due to a phase change for the spirals running through the interstitial atoms alone. It is necessary to assume also a phase difference between the spirals running through the Mn_1 atoms in (a) (Table 2) which in space group $P222_1$ are connected through a symmetry translation. A phase difference of 60° between these spirals accounts well for all the intensity changes which we observe. An improved agreement is also obtained by assuming the spirals through the interstitial atoms to have a phase difference of 30° with that through 0,0,0. However, their contribution is small and this angle must be considered uncertain. A list of the phase angles and the angles which the moments make with the moment at 0,0,0 is given in Table 5.

Normalization leads to a moment value of 2.0 μ_B at 12 K. The obtained agreement between the observed and calculated intensities is shown in Table 4. We cannot claim any high accuracy in this determination since most of the satellites are very weak and the $000^{\pm}$ satellite is riding on a high and sloping background.

Table 5. Phase angles between spirals and moment angles.

	$MnBi_{0.9}Sb_{0.1}$				MnBi quenched	
	12 K		78 K		293 K	
	ϕ	angle with moment at 0,0,0	ϕ	angle with moment at 0,0,0	ϕ	angle with moment at 0,0,0
Mn_1 $x,0,0$	0	0	0	0	0	0
Mn_1' $\bar{x},0,\frac{1}{2}$	60	102	0	42	90	116
Mn_2 $x,\frac{1}{2},0$	–	–	–	–	270	270
Mn_2' $\bar{x},\frac{1}{2},\frac{1}{2}$	–	–	–	–	180	206
Mn(I) $\frac{1}{2},y,\frac{1}{4}$	30	51	0	21	270	283
Mn(I)′ $\frac{1}{2},\bar{y},\frac{3}{4}$	30	93	0	63	90	129

In order to carry out a least squares refinement on the fundamental reflections at 12 K using the profile programme it was essential to subtract the contribution from overlapping satellite peaks. This was done assuming the peaks to have a Gaussian shape with the same half width as the fundamental reflections. The result of the profile refinement is shown as the fully drawn curve in Fig. 2, and the final parameters are given in Table 3. Both the occupation numbers and the position parameters are closely similar to those obtained at 293 K. It was attempted to lower the symmetry by breaking the symmetry relation required by the two-fold screw axis. However, this resulted in a larger R-factor and a lack of convergence of the parameters. No indications were found of any magnetic contribution to the fundamental peaks. The higher R-factor obtained at 12 K over that at 293 K can be attributed to the uncertainty in the satellite contributions. A small ferro- or antiferro-magnetic moment can, however, not be excluded.

To study the temperature variation of the spiral structure the position and intensity of the 000± satellite was recorded as a function of temperature

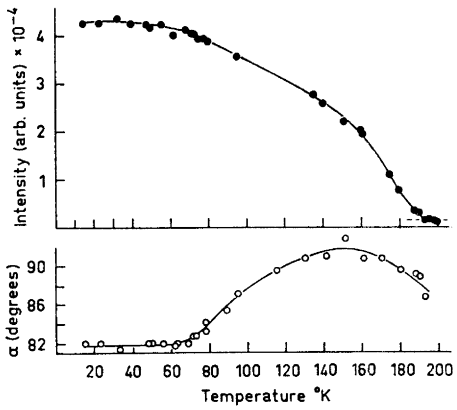

Fig. 3. Above the integrated intensity of the 000± satellite (statistical error less than symbol) and below the spiral turn angle over one unit cell length as a function of temperature for $MnBi_{0.9}Sb_{0.1}$.

from 12 K to 200 K. In Fig. 3 is plotted on top the integrated intensity and below the spiral turn angle, α, over one unit cell length, derived from

$$\alpha = 360° \ \tau/c^*$$

At 12 K the satellite position corresponds to a turn angle of 82.0°. This angle remains unchanged until the temperature approaches 70 K. Then the 2θ angle and the corresponding turn angle start to increase and this continues until α reaches a value of 92.8° at 150 K. From this temperature on the turn angle again decreases. The intensity falls off gradually, but with an apparent change of slope at approximately the same temperatures. Extrapolating to zero a Néel temperature of 195 ± 3 K is found. The satellite position just below this point corresponds to a turn angle of $\alpha = 86.8°$.

RESULTS ON QUENCHED MnBi

The solution of the chemical and magnetic structure of quenched MnBi is considerably more difficult than the former problem due to the low intensity of the superstructure peaks and the magnetic peaks and the presence of a large amount of impurities. However, after having solved the problem of $MnBi_{0.9}Sb_{0.1}$ it became possible by analogy to reach a solution also for this problem.

A neutron diffraction diagram of quenched MnBi obtained at room temperature is shown in Fig. 4. Except for the impurity peaks and a few peaks

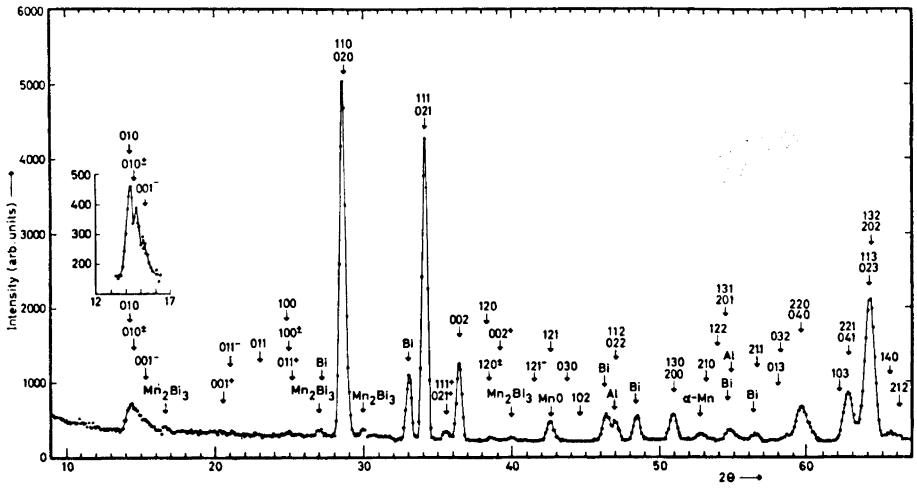

Fig. 4. Neutron diffraction diagram of quenched MnBi obtained at 293 K, $\lambda = 1.863$ Å. The curve is drawn through the experimental points. Insert shows a part of the diagram repeated with better collimation.

which can be considered as satellites to the fundamental peaks, the observed peaks can be indexed on an orthorhombic unit cell of dimensions:

$$a = 4.334(2) \text{ Å} \qquad b = 7.505(4) \text{ Å} \qquad c = 5.959(7) \text{ Å}$$

This unit cell is somewhat larger than the unit cell of $MnBi_{0.9}Sb_{0.1}$, in particular along the c-axis, and is similar to the one for quenched MnBi given in the previous paper,[1] however, with the axes interchanged. The peaks which at that time seemed to require a doubling of two of the axes are now attributed partly to impurities and partly to a spiral structure.

The impurities are in addition to a certain amount of the unquenched phase some unreacted Bi and a small amount of α-Mn and MnO. A few weak peaks can apparently be ascribed to a small amount of the phase Mn_2Bi_3, *i.e.* the orthorhombic phase reported by Fürst and Halla [9] and Halla and Montignié [10] to be present in samples quenched from high temperatures.

A special difficulty was introduced by the presence of a variable amount of the unquenched phase which increased with time after quenching and gave peaks overlapping those of the quenched phase. It was here necessary to estimate the average amount of the unquenched phase during the neutron diffraction run from X-ray diagrams obtained before and after the run. The intensities of the reflections were calculated, and their contribution subtracted point by point assuming a Gaussian shape of the peaks with the same half width as for the quenched phase.

The corrected intensities were used as input in a profile refinement calculation. The space group was again assumed to be $P222_1$ and the possible atomic positions those given in Table 2. Both nuclear and magnetic contributions were calculated and the following parameters refined: the occupation numbers, the position parameters, the scale factor, the overall temperature factor, three half width parameters, the unit cell constants, and the components of the magnetic moments.

As for $MnBi_{0.9}Sb_{0.1}$ it soon turned out that the interstitial atoms, Mn(I), only occupy the (*d*) positions and that the (*c*) positions are empty (Table 2). The Mn-atoms in regular positions are distributed on both the (*a*) and (*b*) sites, but also here with most vacancies on the (*b*) sites. The *x*-parameters of Mn_1 and Mn_2 remained close to 0 and 0.5, respectively, and were kept constant at these values in the final refinements. The other parameters were refined until negligible shifts were obtained, and the result is given in Table 6. The

Table 6. Result of least squares profile refinement on quenched MnBi.

	occ.no.	*x*	*y*	*z*	μ_z
Mn_1 in (*a*)	0.96(5)	0	0	0	1.80(17)
Mn_2 in (*b*)	0.90(5)	$\frac{1}{2}$	$\frac{1}{2}$	0	1.70(19)
Mn(I) in (*d*)	0.33(6)	$\frac{1}{2}$	0.102(17)	$\frac{1}{4}$	1.60(84)
Bi_1 in (*c*)	1.02(4)	0	0.335(3)	$\frac{1}{4}$	
Bi_2 in (*d*)	0.88(3)	$\frac{1}{2}$	0.801(3)	$\frac{1}{4}$	

Overall isotropic $B = 1.11(21)$ Å^2

$R_{nucl} = 4.2$ % $R_{magn} = 4.0$ %

magnetic moments were found to be ferromagnetically aligned along the *c*-axis with an average component in this direction of 1.73 μ_B. Components in other directions were tried, but these did not converge and showed large standard deviations. The average ferromagnetic moment per Mn-atom is in close agreement with the value 1.7 μ_B which was derived from magnetization measurements by Heikes.[2] The *R*-factors obtained are 4.2 % for the nuclear peaks and 4.0 % for the magnetic peaks.

The occupation numbers derived show that 15 % of the Mn-atoms occupy interstitial positions. These are situated in every second layer perpendicular to the *a*-axis (Fig. 1b). It is interesting to note that it is also in these layers that both the Mn and Bi vacancies are concentrated and that the large displacements are found. In the other layers the atomic positions are closely the same as those derived from an undistorted NiAs-type structure.

In contrast to $MnBi_{0.9}Sb_{0.1}$, no change in the diagram was observed on cooling to 12 K. However, a few peaks visible also at room temperature indicated the presence of a spiral component over the whole temperature range. A typical feature of the diagram in Fig. 4 is thus the presence of a shoulder on the high angle side of the 010 peak. This was also visible in the previously published diagram of quenched MnBi (Fig. 6 in Ref. 1). On increasing the resolution the diagram revealed the presence of two additional peaks in this region (see insert in Fig. 4). These can, in analogy to $MnBi_{0.9}Sb_{0.1}$, be identified as the satellite peaks $010^{\pm}$ and 001^{-} due to a spiral propagating along the c^* axis with the propagation vector $0.146\ \vec{c}^*$. For $MnBi_{0.9}Sb_{0.1}$, a strong $000^{\pm}$ peak was also observed. With the present propagation vector this should appear at $2\theta = 2.54°$. However, in spite of a thorough search using narrow collimation it proved impossible to find any peak at small angles. This can be attributed to the presence of a phase difference between the spirals. The most prominent difference between the two structures is that in $MnBi_{0.9}Sb_{0.1}$ the central row of Mn-atoms has been removed, whereas in quenched MnBi this row and that through the corners are not far from being equally populated. If the spirals running through these rows are in opposite phase, only a weak $000^{\pm}$ peak would result.

Except for the overlapping reflections 021^{+} and 111^{+}, all the other satellites are rather weak and uncertain, and it is only possible to arrive at a tentative conclusion for the spiral structure. However, with the computer programme allowing the R factor to be calculated for a series of sets of predetermined phase angles it was possible to arrive at a solution giving a reasonable agreement for all the satellites, also those of zero intensity. The obtained agreement is shown in Table 7. In Table 5 are given both the phase angles of the spirals

Table 7. Satellite intensities from quenched MnBi.

hkl	I_{calc}		I_{obs}
$000^{\pm}$	0.35		–
$010^{\pm}$	23.49	51.49	43
001^{-}	28.00		
001^{+}	7.19		~3
011^{-}	0.76		~3
$100^{\pm}$	6.60	7.00	5
011^{+}	0.40		
111^{+}	9.47	12.66	13
021^{+}	3.19		
$120^{\pm}$	4.53		4
002^{+}	0.00		–
121^{-}	0.01		–

and the angle which each of the moments makes with the moment at 0,0,0. It is seen that it is the spiral through the atom at $\frac{1}{2},\frac{1}{2},\frac{1}{2}$ which is in opposite phase to that through 0,0,0 and the spiral through $\frac{1}{2},\frac{1}{2},0$ which is in opposite phase to that through $0,0,\frac{1}{2}$. The spirals through the interstitial atoms are also in opposite phase to each other. Normalization gives for the spiral component

a moment value of 1.8 μ_B. Together with the ferromagnetic moment of 1.73 μ_B this gives a total moment of 2.50 μ_B. The moments lie on cones with axes along the *c*-axis and an opening angle approximately 90°. It should be stressed that these conclusions are rather tentative, and that the final picture might be much more complicated. We have thus arbitrarily assumed all the atoms to have the same moment value and all the cones to have the same opening angle.

DISCUSSION AND CONCLUSIONS

It has been found that the orthorhombic MnBi phase which is obtained on rapid quenching from above 360°C can be produced as a stable phase at low temperature by the addition of a small amount of Sb. As previously found,[1] the unit cell is the orthohexagonal cell derived from an NiAs-type cell with some of the Mn-atoms occupying interstitial positions. However, contrary to previous expectations an ordering is found to take place both of the Mn-vacancies and the interstitials.

The vacancies are concentrated in the row parallel to the *c*-axis passing through the center of the cell (Fig. 1), and in $MnBi_{0.9}Sb_{0.1}$ this row is even completely empty. Concurrently the interstitials are found to occupy only the positions lying in the plane passing through this row. Thus, both the Mn-vacancies and interstitials are situated in every second layer perpendicular to the *a*-axis.

This is reflected in the observed displacements. In $MnBi_{0.9}Sb_{0.1}$ the absence of the central row has made the interstitials move in towards the centre of the cell ($y = 0.215$) (Table 3), whereas in quenched MnBi they have been pushed outwards ($y = 0.102$) (Table 6). In an undistorted NiAs-type lattice this coordinate would be $y = 0.167$. Similarly it is seen that in $MnBi_{0.9}Sb_{0.1}$ the absence of the central row has made the Bi/Sb-atoms move close together.

In $MnBi_{0.9}Sb_{0.1}$ a large number of vacancies are found also in the Bi/Sb positions. These are distributed about evenly over all the Bi/Sb sites. In quenched MnBi, however, the Bi-vacancies are concentrated in the layers containing the Mn-vacancies and interstitials. From the sum of the occupation numbers it appears that the sample $MnBi_{0.9}Sb_{0.1}$ has a close to equiatomic composition whereas the quenched MnBi used here has an excess of Mn-atoms of approximately 7 atomic %. It should be noted that in the last case the number of interstitial Mn-atoms, 15 atomic %, is exactly the same as that previously[1] reported to be present in the high temperature paramagnetic phase of MnBi.

The interatomic distances are listed in Table 8 with the numbering of the atoms as given in Tables 2 and 5. The Mn-atoms in the fully occupied rows are surrounded by distorted octahedra of Bi-atoms with two at a distance of 3.04 Å and four at a distance of 3.00 Å in $MnBi_{0.9}Sb_{0.1}$. In quenched MnBi the corresponding distances are 2.92 Å and 3.02 Å, while the Bi-octahedra surrounding the central row of Mn-atoms have the shorter distances 2.71 Å and 2.91 Å. This can be correlated with the tendency of the Mn-atoms to leave the central row. The displacement of the interstitial atoms from the centre of the bipyramidal holes has led to some very short Mn – Bi distances.

Table 8. Interatomic distances in Å.

	$MnBi_{0.9}Sb_{0.1}$		MnBi quenched
	12 K	293 K	293 K
Mn_1-Mn_1'	2.86	2.87	2.98
$Mn_1-Mn(I)$	3.01	3.04	2.74
$Mn_2-Mn(I)$	–	–	3.34
Mn_1-Bi_1	3.03	3.04	2.92
Mn_1-Bi_2	2.98	3.00	3.02
Mn_2-Bi_2	–	–	2.71
Mn_2-Bi_1	–	–	2.91
$Mn(I)-Bi_2$	2.86	2.87	3.07
$Mn(I)-Bi_2'$	3.06	3.12	2.26
$Mn(I)-Bi_1$	2.41	2.40	2.78
Bi_1-Bi_1'	3.52	3.56	3.88
Bi_1-Bi_2	3.76	3.77	3.82

In $MnBi_{0.9}Sb_{0.1}$ the absence of the central row of Mn-atoms has made the interstitials move in towards the centre of the cell leading to two very short Mn – Bi distances of 2.40 Å. However, of the positions in question only 38 % of the Mn-positions and 69 % of the Bi-positions are occupied. In quenched MnBi the interstitials have been pushed in the opposite direction leading to one very close Mn – Bi contact of 2.26 Å. In this case 33 % of the Mn-positions and 88 % of the Bi-positions are occupied. Similar short distances for the interstitial metal atoms in filled up NiAs-type structures have been found in the phases $T_{1+x}Sb$ (T = Cr, Mn, Fe, Co, Ni) by Kjekshus and Walseth.[15] The short Mn – Mn distance 2.74 Å in quenched MnBi is in agreement with a low spin state for the Mn-atoms.[16] The shortest Bi – Bi distance in quenched MnBi is 3.82 Å whereas in $MnBi_{0.9}Sb_{0.1}$ the substitution with Sb has diminished this to 3.56 Å.

Magnetization measurements have shown both samples to be ferromagnetic at room temperature, but with a much larger moment in quenched MnBi than in $MnBi_{0.9}Sb_{0.1}$. Due to the presence of impurities no attempt was made to derive moment values from these measurements. However, from the diffraction data on quenched MnBi a ferromagnetic component of 1.73 μ_B per Mn-atom was deduced in excellent agreement with the value, 1.7 μ_B, obtained from magnetization measurements by Heikes.[2] In $MnBi_{0.9}Sb_{0.1}$ no ferromagnetic component could be found and the weak ferromagnetism observed is attributed to the presence of a small amount of the ferrimagnetic compound Mn_2Sb.

In $MnBi_{0.9}Sb_{0.1}$ moments with a saturation value of 2.0 μ_B form a spiral along the *c*-axis with the propagation vector 0.228 $\vec{c}^*$. This corresponds to a spiral turn angle of 82° over one unit cell length. While this angle and the corresponding satellite positions remain the same from 12 K to about 70 K, the intensity of some of the satellites varies drastically. We attribute this to a change in the phase relation between the spirals. At 78 K the satellite intensities correspond to a situation in which all the spirals are in phase, whereas at 12 K the intensities require a phase difference even between spirals running

through atoms which are related by symmetry. A corresponding lowering of the crystallographic symmetry could not be inferred from our data.

From 70 K to about 150 K there is a gradual increase in the spiral turn angle and from then on a gradual fall off. At the same temperatures a change of slope seems to appear in the intensity *versus* temperature curve. The Néel point is found to be 195 ± 3 K (Fig. 3).

In quenched MnBi the spiral propagation vector $0.146\ \vec{c}^*$ is much shorter corresponding to a spiral turn angle of 52.6° over one unit cell length. No change appears to take place with temperature. However, the accuracy of the data is not sufficient to allow any definite conclusion on this point. The phase angles given in Table 5 must also be considered rather tentative. From the angles which the moments make with the moment at 0,0,0 it appears that the moments at Mn_1' and (Mn(I)' which are separated by the short distance 2.74 Å are approximately parallel. These moments are also close to parallel in $MnBi_{0.9}Sb_{0.1}$, where their distance is 3.04 Å. Similarly the moments on Mn_2 and Mn(I) which are separated by 3.34 Å are approximately parallel. It seems reasonable to attribute this to a ferromagnetic superexchange coupling similar to the one which is responsible for the strong ferromagnetic property of annealed MnBi. However, in this case it cannot be ascribed to a quasistatic Jahn-Teller effect as proposed by Goodenough [17] since the Mn^{3+} ions appear to be in a low spin state. Goodenough has pointed out that the competition with the direct cation-cation interaction along the *c*-axis which is antiferromagnetic may lead to a spiral structure. This is apparently what is happening here. The importance of this direct interaction increases as we go from annealed MnBi to quenched MnBi and finally to $MnBi_{0.9}Sb_{0.1}$ since the Mn – Mn distance along the *c*-axis decreases from 3.06 Å to 2.98 Å and finally to 2.87 Å. Correspondingly we observe a transition from a pure ferromagnet to a pure helimagnet.

The spiral component at room temperature in quenched MnBi is 1.8 μ_B which together with the ferromagnetic component gives a total moment of 2.50 μ_B per Mn-atom making an angle of approximately 45° with the *c*-axis. In $MnBi_{0.9}Sb_{0.1}$ a saturation moment of 2.0 μ_B was deduced. This is in agreement with a low spin state assuming Mn^{3+} ions. However, the difference between the values indicates the need of applying a band model.

REFERENCES

1. Andresen, A. F., Hälg, W., Fischer, P. and Stoll, E. *Acta Chem. Scand.* **21** (1967) 1543.
2. Heikes, R. R. *Phys. Rev.* **99** (1955) 446.
3. Wilson, R. H. and Kasper, J. S. *Acta Cryst.* **17** (1964) 95.
4. Grønvold, F., Snildal, S. and Westrum, E. F., Jr. *Acta Chem. Scand.* **24** (1970) 285.
5. Goodenough, J. B., Ridgley, D. H. and Newman, W. A. *Proc. Nottingham Conf. on Magnetism* (1964) 542.
6. Goodenough, J. B. and Kafalas, J. A. *Phys. Rev.* **157** (1967) 389.
7. Rietveld, H. M. *J. Appl. Cryst.* **2** (1969) 65.
8. Cornish, A. J. *U. S. Patent Application No. 446945*, filed July 30, 1954.
9. Fürst, U. and Halla, F. *Z. physik. Chem. (Leipzig)* **B 40** (1938) 285.
10. Halla, F. and Montignié, E. *Z. physik. Chem. (Leipzig)* **B 42** (1939) 153.

11. Dannöhl, H.-D. and Gmöhling, W. *Z. Metallk.* **54** (1963) 564.
12. Begum, R. J. and Satya Murthy, N. S. *Bahba Atomic Research Centre Report B.A.R.C.* – 394 (1969).
13. Neutron Diffraction Commission, *Acta Cryst.* **A 25** (1969) 391.
14. Watson, R. E. and Freeman, A. J. *Acta Cryst.* **14** (1961) 27.
15. Kjekshus, A. and Walseth, K. P. *Acta Chem. Scand.* **23** (1969) 2621.
16. Pearson, W. B. *Z. Krist.* **126** (1968) 362.
17. Goodenough, J. B. *Magnetism and the Chemical Bond*, Interscience, New York 1963.

Received April 1, 1971.